Research Article

A Computationally Efficient Optimal Wigner Distribution in LCT Domains for Detecting Noisy LFM Signals

An-Yang Wu [ID],[1] **Xi-Ya Shi** [ID],[1] **Yun Sun** [ID],[1] **Xian Jiang** [ID],[1] **Sheng-Zhou Qiang** [ID],[1] **Pu-Yu Han** [ID],[1] **Yun-Jie Chen** [ID],[1] **and Zhi-Chao Zhang** [ID][1,2]

[1]*School of Mathematics and Statistics, Nanjing University of Information Science and Technology, Nanjing 210044, China*
[2]*Faculty of Information Technology, Macau University of Science and Technology, Macau 999078, China*

Correspondence should be addressed to Zhi-Chao Zhang; zzc910731@163.com

Recently, Wigner distribution (WD) associated with linear canonical transforms (LCTs) is quickly becoming a promising technique for detecting linear frequency-modulated (LFM) signals corrupted with noises by establishing output signal-to-noise ratio (SNR) inequality model or optimization model. Particularly, the closed-form instantaneous cross-correlation function type of WD (CICFWD), a unified linear canonical Wigner distribution, has shown to be competitive in detecting noisy LFM signals under an extremely low SNR. However, the CICFWD has up to nine LCT free parameters so that it requires a heavy computational load. To improve the efficiency of real-time processing, this paper focuses on the instantaneous cross-correlation function type of WD (ICFWD), which has only six LCT free parameters but is not a special case of the CICFWD. The main advantage of ICFWD is that it could be expected to reduce the computational complexity while maintaining detection performance. This paper first proposes an optimization model to the ICFWD's output SNR with respect to deterministic signals embedded in additive zero-mean noises. It then deduces the model's solution to a single component LFM signal added with white noise, leading to the optimal selection strategy on LCT free parameters. Simulation results demonstrate that the ICFWD improves almost a doubling of computing speed in comparison with the CICFWD while sharing the same level of detection performance. To be specific, the computing time of ICFWD in sampling frequencies 5 Hz, 10 Hz, 15 Hz, and 20 Hz is about 0.048 s, 0.111 s, 0.226 s, and 0.392 s, respectively, while 0.075 s, 0.233 s, 0.478 s, and 0.821 s for the computing time of CICFWD; the ICFWD and CICFWD have nearly the same output SNR higher than that of the WD.

1. Introduction

Linear canonical transform (LCT) [1–4], also known as ABCD transform, affine Fourier transform, and lossless first-order optical transform, was used to solve differential equations and analyze optical models in the early years [5]. The LCT has three free parameters, which enable it to be capable of providing a mathematical model for paraxial propagation through quadratic phase systems [6–8]. It can also be described and characterized by propagation through free space in the Fresnel approximation or through sections of graded-index media, implemented with an arbitrary number of thin lenses [6–8]. From the viewpoint of time-frequency analysis, thanks to more degrees of freedom, the

LCT outperforms the ordinary Fourier transform (FT) which is subjected to the time or the frequency domain representation, giving a flexible nonstationary signal representation in time-frequency domains.

Wigner distribution (WD) [9–11] is the generating distribution for Cohen's class time-frequency representations [12]. It can be suitable in the process of linear frequency-modulated (LFM) signals, which are frequently encountered in many engineering applications such as satellite communications [13] and synthetic aperture radar (SAR) [14]. However, in the case of extremely strong noise interference, the WD fails to provide enough signal representation flexibility to extract the signal from the noise. To address this shortcoming, a promising technique that

introduces LCT free parameters into the traditional WD has attracted much attention in recent years.

Indeed, as early as 2001, Pei and Ding [15] presented the affine characteristic type of WD (ACWD) to separate multicomponent signals through the designing of filters in LCT domains, which is none other than the traditional WD affinely transforming in the time-frequency plane. Until 2012, Bai et al. [16] proposed the kernel function type of WD (KFWD), which differs essentially from the traditional WD, by replacing the kernel function of the FT with that of the LCT. In consideration of the fact that the KFWD is subjected to the conventional energy domain representation when dealing with LFM signals, in 2016 Zhang [17] proposed the convolution representation type of WD (CRWD) by replacing the classical convolution operator with a general form in the LCT domain. To combine the advantages of energy domain and correlation domain representations, Zhang [18] also proposed the instantaneous cross-correlation function type of WD (ICFWD) [19] to integrate the WD and the ambiguity function. Two different LCT parameter matrices embedded in the ICFWD are acting, respectively, on the signal and the kernel function, indicating that the ICFWD is a six-free-parameter class of bilinear time-frequency distribution.

In order to unify the existing Wigner distributions in LCT domains, such as the ACWD, KFWD, CRWD, and ICFWD, Zhang and Luo [20] proposed the closed-form instantaneous cross-correlation function type of WD (CICFWD) [19] by applying also another LCT parameter matrix on the signal's complex conjugate. The CICFWD has been shown to be the main body of Wigner distributions in LCT domains, and it achieves a good detection performance under some LCT free parameters while a poor one in other cases. To disclose a causal relationship between appropriate parameters and good detection effects, the function of output signal-to-noise ratio (SNR) with respect to parameters was investigated. The CICFWD's expectation-SNR [21, 22] and variance-SNR [8, 19] defined, respectively, by the ratio of magnitude spectrums and energy spectrums are currently derived. Output SNR inequality [21]/inequalities system [8] model and optimization [22]/multiobjective optimization [19] model are then established to reveal the underlying mechanism of the improvement of detection effects triggered by the LCT free parameters. However, the CICFWD has as many as nine parameters so that its implementation requires a high computation cost, which is unbearable to most real-time information analysis problems, such as real-time communication processing and real-time SAR imaging.

Compared with the CICFWD, the ICFWD has few LCT free parameters but is not a special case. It is this fact that enables the ICFWD to be more computationally efficient while maintaining the same level of detection performance as the CICFWD. Thus, the main research object of this paper is the ICFWD. In the paper, we first formulate the ICFWD's expectation-SNR definition for a generalized noisy signal expression and establish an output SNR optimization model of the ICFWD. We then make a strategic decision on the optimal parameters by solving the optimization model with

respect to a single component LFM signal embedded in additive white noise. We also compare the computing speed and detection performance of ICFWD and CICFWD through numerical experiments.

The main contributions of this paper are summarized as follows:

(i) It defines the expectation-SNR of ICFWD for a generalized noisy signal consisting of signal and additive zero-mean noise

(ii) It constructs the output expectation-SNR optimization model of ICFWD on the generalized noisy signal

(iii) It obtains the solution of the optimization model for analytic single component LFM signal added with white noise

(iv) It reveals the competitive strengths of ICFWD in maintaining detection performance and saving computing time as compared with the CICFWD

The remainder of this paper is structured as follows: Section 2 collects some background knowledge of the LCT and ICFWD; Section 3 studies the optimization modeling and solving of the output SNR of ICFWD; Section 4 deduces the optimal selection strategy on LCT free parameters for a single component LFM signal embedded in additive white noise; Section 5 conducts numerical experiments; and Section 6 concludes the paper and demonstrates the future research interests.

2. Preliminaries

2.1. LCT. The LCT includes the classical FT, the Fresnel transform, the Lorentz transform, the fractional Fourier transform [23–27], and the scaling and chirp multiplication operators [28] as special cases. The LCT's generality enables it to be capable of solving many mathematical, physical, and engineering problems that other conventional transformations fail to solve. For a signal $f(t)$, its LCT associated with the parameter matrix $\mathbf{A} = (a, b; c, d)$ is given by [29–35]

$$F_{\mathbf{A}}(u) = \begin{cases} \int_{-\infty}^{+\infty} f(t)\mathscr{K}_{\mathbf{A}}(u, t)\mathrm{d}t, & b \neq 0, \\ \sqrt{d}\, e^{j(c\, d)/2u^2} f(\mathrm{d}u), & b = 0, \end{cases} \tag{1}$$

where

$$\mathscr{K}_{\mathbf{A}}(u, t) = \frac{1}{\sqrt{j2\pi b}} e^{j\left(d/(2b)u^2 - (1/b)ut + a/(2b)t^2\right)} \tag{2}$$

denotes the LCT kernel function, and where a, b, c, d are LCT real parameters that satisfy $a\, d - bc = 1$.

The variable u in the kernel function and the LCT domain are abbreviated as the linear canonical frequency and the linear canonical domain, respectively.

As it is seen, the LCT is just a type of scaling and chirp multiplication operations for $b = 0$. We, therefore, have no interest in dealing with this particular case. Without loss of generality, this paper focuses only on the LCT with $b \neq 0$,

from which a relation $c = (ad - 1)/b$ derives. In this case, three free parameters of the LCT are none other than a, b, d.

2.2. ICFWD.

For a signal $f(t)$, its CICFWD associated with parameter matrices $\mathbf{A}_1 = (a_1, b_1; c_1, d_1)$, $\mathbf{A}_2 = (a_2, b_2; c_2, d_2)$, and $\mathbf{A} = (a, b; c, d)$ is defined by [6, 8, 19–22]

$$W_f^{\mathbf{A}_1, \mathbf{A}_2, \mathbf{A}}(t, u) = \int_{-\infty}^{+\infty} F_{\mathbf{A}_1}\left(t + \frac{\tau}{2}\right) F_{\mathbf{A}_2}^*\left(t - \frac{\tau}{2}\right) \mathscr{K}_{\mathbf{A}}(u, \tau) \mathrm{d}\tau, \tag{3}$$

where the superscript $*$ stands for a complex conjugate operator, $F_{\mathbf{A}_1}$ and $F_{\mathbf{A}_2}$ stand for LCTs of $f(t)$ associated with parameter matrices $\mathbf{A}_1$ and $\mathbf{A}_2$, respectively, and $\mathscr{K}_{\mathbf{A}}(u, \tau)$ stands for the LCT kernel function associated with the parameter matrix $\mathbf{A}$.

As shown in the definition of CICFWD, there exist three different matrices $\mathbf{A}_1$, $\mathbf{A}_2$, and $\mathbf{A}$, i.e., nine LCT free parameters. Although the CICFWD is particularly suitable for noisy LFM signals detection, it is computationally expensive. A wise alternative is thus the ICFWD, which has only six parameters. For a signal $f(t)$, its ICFWD associated with parameter matrices $\mathbf{A}_1$ and $\mathbf{A}$ is defined by [18]

$$W_f^{\mathbf{A}_1, \mathbf{A}}(t, u) = \int_{-\infty}^{+\infty} F_{\mathbf{A}_1}\left(t + \frac{\tau}{2}\right) f^*\left(t - \frac{\tau}{2}\right) \mathscr{K}_{\mathbf{A}}(u, \tau) \mathrm{d}\tau. \tag{4}$$

Because of $b_2 \neq 0$, $F_{\mathbf{A}_2}$ does not reduce to f at any time, implying that the ICFWD is by no means a special case of the CICFWD.

It should also be noted that in the case of $\mathbf{A}_1 = (1, 0; 0, 1)$ and $\mathbf{A} = (0, 1; -1, 0)$ the ICFWD turns into the conventional WD [10]

$$W_f(t, \omega) = \int_{-\infty}^{+\infty} f\left(t + \frac{\tau}{2}\right) f^*\left(t - \frac{\tau}{2}\right) e^{-j\omega\tau} \mathrm{d}\tau. \tag{5}$$

3. ICFWD's Output SNR Optimization Modeling and Solving

This section first defines the output SNR of ICFWD according to the mathematical expectation result on a generalized noisy signal expression. It then introduces the ICFWD's output SNR optimization model. It also summarizes the solving process of optimization problems by considering analytic and nonanalytic noisy signals, respectively.

3.1. Expectation-SNR Definition of ICFWD.

For a generalized noisy signal expression $f(t) + n(t)$, where $f(t)$ and $n(t)$ denote a deterministic signal and a zero-mean noise (if its mean were not zero, one could normalize the mean as zero), respectively, the mathematical expectation of ICFWD reads

$$E\left[W_{f+n}^{\mathbf{A}_1, \mathbf{A}}(t, u)\right] = W_f^{\mathbf{A}_1, \mathbf{A}}(t, u) + E\left[W_n^{\mathbf{A}_1, \mathbf{A}}(t, u)\right]. \tag{6}$$

See Appendix A for the proof of the above formula. Similar to the CICFWD's output SNR definition given by

([21], equation (32) or [22], equation (6)), the expectation-SNR of ICFWD is well defined as

$$\mathrm{ESNR}_{\mathrm{ICFWD}}^{\mathbf{A}_1, \mathbf{A}} = \frac{\max\limits_{(t,u)\in\mathbb{R}^2}\left|W_f^{\mathbf{A}_1, \mathbf{A}}(t, u)\right|}{\underset{\arg\max\limits_{(t,u)}|W_f^{\mathbf{A}_1, \mathbf{A}}(t, u)|}{\mathrm{Mean}}\left\{\left|E\left[W_n^{\mathbf{A}_1, \mathbf{A}}(t, u)\right]\right|\right\}}, \tag{7}$$

where "Mean" stands for the arithmetic mean when $\arg\max_{(t,u)}|W_f^{\mathbf{A}_1, \mathbf{A}}(t, u)|$ is a countable set while the integral average when it is an uncountable set.

3.2. ICFWD's Output SNR Optimization Modeling.

As shown in (7), for given signals and noises the expectation-SNR of ICFWD relies on a combination of double matrixes $\mathbf{A}_1$, $\mathbf{A}$. A natural idea is then to explore the optimal combination that reaches the maximum value of expectation-SNR. By taking the expectation-SNR and LCT free parameters as an objective function and decision variables, respectively, there is an optimization model for the output SNR of the ICFWD

$$\max_{\mathbf{A}_1, \mathbf{A}} \mathrm{ESNR}_{\mathrm{ICFWD}}^{\mathbf{A}_1, \mathbf{A}}. \tag{8}$$

3.3. ICFWD's Output SNR Optimization Solving.

It does not seem workable to solve the optimization model (8) in a common way as the objective function relies heavily on the deterministic signal and the noise. It should also be emphasized that solutions of (8) differ in analytic and nonanalytic noisy signal expressions. Moreover, it requires a lower computation cost to solve the ICFWD's output SNR optimization model as compared with solving that of the CICFWD.

3.3.1. Analytic Case.

For analytic noisy signals, $W_f^{\mathbf{A}_1, \mathbf{A}}(t, u)$ and $W_n^{\mathbf{A}_1, \mathbf{A}}(t, u)$ can be seen as bivariate parametric functions of variables t, u and parameter matrices $\mathbf{A}_1$, $\mathbf{A}$. By using the classical extreme value theory [36], $\max_{(t,u)\in\mathbb{R}^2}|W_f^{\mathbf{A}_1, \mathbf{A}}(t, u)|$ can be simplified as an algebraic expression associated with six LCT free parameters. Then $\mathrm{Mean}_{\arg\max_{(t,u)}|W_f^{\mathbf{A}_1, \mathbf{A}}(t, u)|}\left\{|E[W_n^{\mathbf{A}_1, \mathbf{A}}(t, u)]|\right\}$ can be calculated as another algebraic expression associated with parameters. By substituting these two algebraic expressions into (7), it follows that $\mathrm{ESNR}_{\mathrm{ICFWD}}^{\mathbf{A}_1, \mathbf{A}}$ is a function of six parameters. Since the parameters that give rise to the maximum of ICFWD are subjected to some equality constraints, the optimization model (8) is converted to a conditional extremum problem. Thanks to the Lagrangian multiplier method [37], by taking the Lagrange function's partial derivatives in regard to LCT free parameters, there is a set of algebraic equations. Thus, solving equations yields the optimal parameters. Note that the expectation-SNR of CICFWD is a function of nine parameters. The system of algebraic equations derived from the Lagrangian multiplier method contains more equations than the previous one, and it seems more difficult to solve them.

3.3.2. Nonanalytic Case. For nonanalytic noisy signals, using peak detection algorithms [38] gives a solution to $\max_{(t,u)\in\mathbb{R}^2}|W_f^{\mathbf{A}_1,\mathbf{A}}(t,u)|$ for the given LCT free parameters; $\text{Mean}_{\arg\max_{(t,u)}|W_f^{\mathbf{A}_1,\mathbf{A}}(t,u)|}\{|E[W_n^{\mathbf{A}_1,\mathbf{A}}(t,u)]|\}$ can be calculated from the set of peak points. It then follows a value of $\text{ESNR}_{\text{ICFWD}}^{\mathbf{A}_1,\mathbf{A}}$. By using uniform design [39], traversing representative experimental points and ranking the value thus reach the maximum value, i.e., the maximum expectation-SNR. The corresponding experimental points are just the optimal LCT free parameters. Due to an additional parameter matrix $\mathbf{A}_2$ for the CICFWD, the order of representative experimental points' number is higher than the previous one, resulting in a more expensive computation cost.

4. Optimal LCT Free Parameters for Analytic Single Component LFM Signal Embedded in Additive White Noise

This section explores the optimal selection strategy on the ICFWD's LCT free parameters for an analytic single component LFM signal embedded in additive white noise through the framework of output SNR optimization modeling and solving.

In order to obtain the optimal strategy, the critical step is to translate the ICFWD's expectation-SNR into a function of LCT free parameters. It is necessary to achieve two preparatory results, including the ICFWDs of single component LFM signal and white noise.

4.1. ICFWD of the Single Component LFM Signal. Here is an analytic single component LFM signal

$$f(t) = e^{j\left(\alpha t + \beta t^2\right)}, \tag{9}$$

where the frequency rate $\beta \neq 0$.

In view of equation (4.1) introduced in [18], the ICFWD of (9) is none other than an impulse function

$$\sqrt{2\pi|bh_1|}\delta\left[u - b\left(\frac{d_1 - h_1}{2b_1} + \beta\right)t - \frac{\alpha}{2}b(h_1 + 1)\right], \tag{10}$$

where δ stands for Dirac delta operator, iff LCT free parameters satisfy $(1/h_1) \triangleq 2\beta b_1 + a_1 \neq 0$ and

$$\frac{a}{2b} + \frac{d_1 - h_1}{8b_1} - \frac{\beta}{4} = 0. \tag{11}$$

As it is seen, the ICFWD reaches its maximum at a straight line $u - b((d_1 - h_1)/(2b_1) + \beta)t - (\alpha/2)b(h_1 + 1) = 0$ in (t,u) plane. The optimization problem $\max_{(t,u)\in\mathbb{R}^2}|W_f^{\mathbf{A}_1,\mathbf{A}}(t,u)|$ thus has analytic solutions

$$\underset{(t,u)}{\arg\max}\left|W_f^{\mathbf{A}_1,\mathbf{A}}(t,u)\right| = \left\{(t,u)|u - b\left(\frac{d_1 - h_1}{2b_1} + \beta\right)t - \frac{\alpha}{2}b(h_1 + 1) = 0\right\}, \tag{12}$$

$$\underset{(t,u)\in\mathbb{R}^2}{\max}\left|W_f^{\mathbf{A}_1,\mathbf{A}}(t,u)\right| = \sqrt{2\pi|bh_1|}. \tag{13}$$

4.2. ICFWD of the White Noise. Let D denote the power spectral density of white noise. By using the stationarity of white noise, i.e., $E[n(t_1)n^*(t_2)] = D\delta(t_1 - t_2)$, and using the sifting property of Delta function, i.e., $g(\tau) = \int_{-\infty}^{+\infty} g(t)\delta(t - \tau)\mathrm{d}t$, the ICFWD of $n(t)$ takes

$$E\left[W_n^{\mathbf{A}_1,\mathbf{A}}(t,u)\right] = \frac{D}{2\pi\sqrt{jb_1}\sqrt{jb}}e^{jd/(2b)u^2}e^{j(a_1+d_1-2)/(2b_1)t^2}\int_{-\infty}^{+\infty}e^{j\left((a_1+d_1+2)/(8b_1) + \frac{a}{2b}\right)\tau^2}e^{j((d_1-a_1)/(2b_1)t - u/b)\tau}\mathrm{d}\tau. \tag{14}$$

Thanks to a celebrated relation

$$\int_{-\infty}^{+\infty} e^{pt^2+qt}\mathrm{d}t = \sqrt{\frac{\pi}{-p}}e^{-q^2/(4p)} \ (p \neq 0, \text{Re}(p) \leq 0), \tag{15}$$

taking a module on both sides of (14) gives

$$\left|E\left[W_n^{\mathbf{A}_1,\mathbf{A}}(t,u)\right]\right| = D\sqrt{\frac{2}{\pi|b(a_1 + d_1 + 2) + 4ab_1|}}, \tag{16}$$

for $(a_1 + d_1 + 2)/b_1 \neq -(4a/b)$. Note that the right-hand side of (16) is a constant independent of variables t, u. Its detailed derivation is given in Appendix B. Owing to (11),

the formulation $b(a_1 + d_1 + 2) + 4ab_1$ can be simplified as $b(h_1 + 1)^2/h_1$. Then there is

$$\underset{\underset{(t,u)}{\arg\max}|W_f^{\mathbf{A}_1,\mathbf{A}}(t,u)|}{\text{Mean}}\left\{\left|E\left[W_n^{\mathbf{A}_1,\mathbf{A}}(t,u)\right]\right|\right\} = \frac{D}{|h_1 + 1|}\sqrt{\frac{2}{\pi}\left|\frac{h_1}{b}\right|}, \tag{17}$$

for $h_1 + 1 \neq 0$.

4.3. Solution of the Optimization Model. Substituting (13) and (17) into (7) gives

$$\mathrm{ESNR}_{\mathrm{ICFWD}}^{\mathbf{A}_1,\mathbf{A}} = \frac{\pi}{D}\left|b(h_1+1)\right|, \tag{18}$$

which is a function of parameters a_1, b_1, b. With an equality constraint (11), the optimization model (8) can be converted to the following conditional extremum problem:

$$\text{maximize}\, f(a_1, b_1, b) = b^2(h_1+1)^2,$$

$$\text{subject to}\, g(a_1, b_1, b) = \frac{a}{2b} + \frac{d_1-h_1}{8b_1} - \frac{\beta}{4}. \tag{19}$$

By using the Lagrangian multiplier method, the Lagrange function follows

$$\mathscr{L}(a_1, b_1, b, \lambda) = f(a_1, b_1, b) + \lambda g(a_1, b_1, b), \tag{20}$$

and subsequently, by taking its partial derivatives, there is a set of algebraic equations

$$\begin{cases} \dfrac{\partial \mathscr{L}}{\partial a_1} = 0, \\[2mm] \dfrac{\partial \mathscr{L}}{\partial b_1} = 0, \\[2mm] \dfrac{\partial \mathscr{L}}{\partial b} = 0, \\[2mm] \dfrac{\partial \mathscr{L}}{\partial \lambda} = 0. \end{cases} \tag{21}$$

By solving equations, there are equalities

$$h_1 = d_1$$
$$= \frac{4a}{b}b_1 - 1, \tag{22}$$

$$\frac{2a}{b} = \beta, \tag{23}$$

which can be regarded as the optimal strategy on LCT free parameters. For the detailed proof, ones can refer to Appendix C.

By substituting $h_1 = (4a/b)b_1 - 1$ into (18), the ICFWD's maximum expectation-SNR takes $(\pi/D)|4ab_1|$. As it is known, the maximum expectation-SNR of the traditional WD is $(2\pi/D)$ [22]. Certainly, the former should be greater than the latter in order to achieve a better detection performance. Thus, there is a potential inequality constraint

$$\left|ab_1\right| > \frac{1}{2}. \tag{24}$$

For simplicity, in real-world applications the optimal LCT free parameters are chosen as $a_1 = b/(4-b) - (2\beta/a)$, $b_1 = (1/a)$, $d_1 = (4/b) - 1$, and $(2a/b) = \beta$ satisfying (22)–(24).

5. Numerical Experiments

This section presents simulations to compare the computing speed and detection performance of ICFWD and CICFWD.

Here is the simulated single component LFM signal $f_1(t)$ added with a complex white Gaussian noise $n(t)$

$$f(t) = f_1(t) + n(t)$$
$$= e^{j(t+0.5t^2)} + n(t), |t| \le 5s. \tag{25}$$

Let $\mathrm{Var}[n(t)]$ denote the variance of the noise, which is closely related to the noise's power spectral density D and the noise's bandwidth W, i.e., $\mathrm{Var}[n(t)] = D \times W$. Then the input SNR takes

$$\mathrm{SNR} = 10\log_{10}\frac{\int_{-5}^{5}\left|f_1(t)\right|^2 \mathrm{d}t}{D \times W}. \tag{26}$$

Moreover, the sampling frequency takes 20 Hz.

Figure 1 compares the detection performance of ICFWD with that of CICFWD and WD. The ICFWD and its contour picture are plotted in Figures 1(a) and 1(b), respectively. The CICFWD and its contour picture are plotted in Figures 1(c) and 1(d), respectively. The WD and its contour picture are plotted in Figures 1(e) and 1(f), respectively. The optimal LCT free parameters are selected for $\mathbf{A}_1 = (-1, 2; -1, 1)$ and $\mathbf{A} = (1/2, 2; -3/4, -1)$ obeying the proposed strategy $a_1 = b/(4-b) - (2\beta/a)$, $b_1 = (1/a)$, $d_1 = (4/b) - 1$, and $(2a/b) = \beta$ for the ICFWD and are chosen as $\mathbf{A}_1 = (3/2, 1; -1, 0)$, $\mathbf{A}_2 = (11/6, -1; 1, 0)$, and $\mathbf{A} = (1, 5/2; -4/15, 1/3)$ obeying the optimal strategy introduced in [22] for the CICFWD. By comparing the sharpness of energy straight lines, it is obvious that the detection performance of ICFWD is similar to that of CICFWD, outperforming the detection performance of the traditional WD.

By using Radon transform (RT) [40] to accumulate energy straight lines, it allows conducting a further detection performance comparison through the maximum output of the matched filtering in accordance with the signal. The RT-based CICFWD (RCICFWD) and RT-based WD (RWD) are reproduced here as ([21], equations (53) and (54))

$$\chi_{\mathrm{RCICFWD}}(k,l) = \int\int_{-\infty}^{+\infty}\left|W_f^{\mathbf{A}_1,\mathbf{A}_2,\mathbf{A}}(t,u)\right|^2 \times \delta\left[u - b\left(\frac{d_1 - 1/(2kb_1+a_1)}{2b_1} + \frac{d_2 - 1/(2kb_2+a_2)}{2b_2}\right)t - \frac{l}{2}b\left(\frac{1}{2kb_1+a_1} + \frac{1}{2kb_2+a_2}\right)\right]\mathrm{d}t\mathrm{d}u,$$

$$\chi_{\mathrm{RWD}}(k,l) = \int\int_{-\infty}^{+\infty}\left|W_f(t,\omega)\right|^2 \delta(\omega - 2kt - l)\mathrm{d}t\mathrm{d}\omega,$$

$$\tag{27}$$

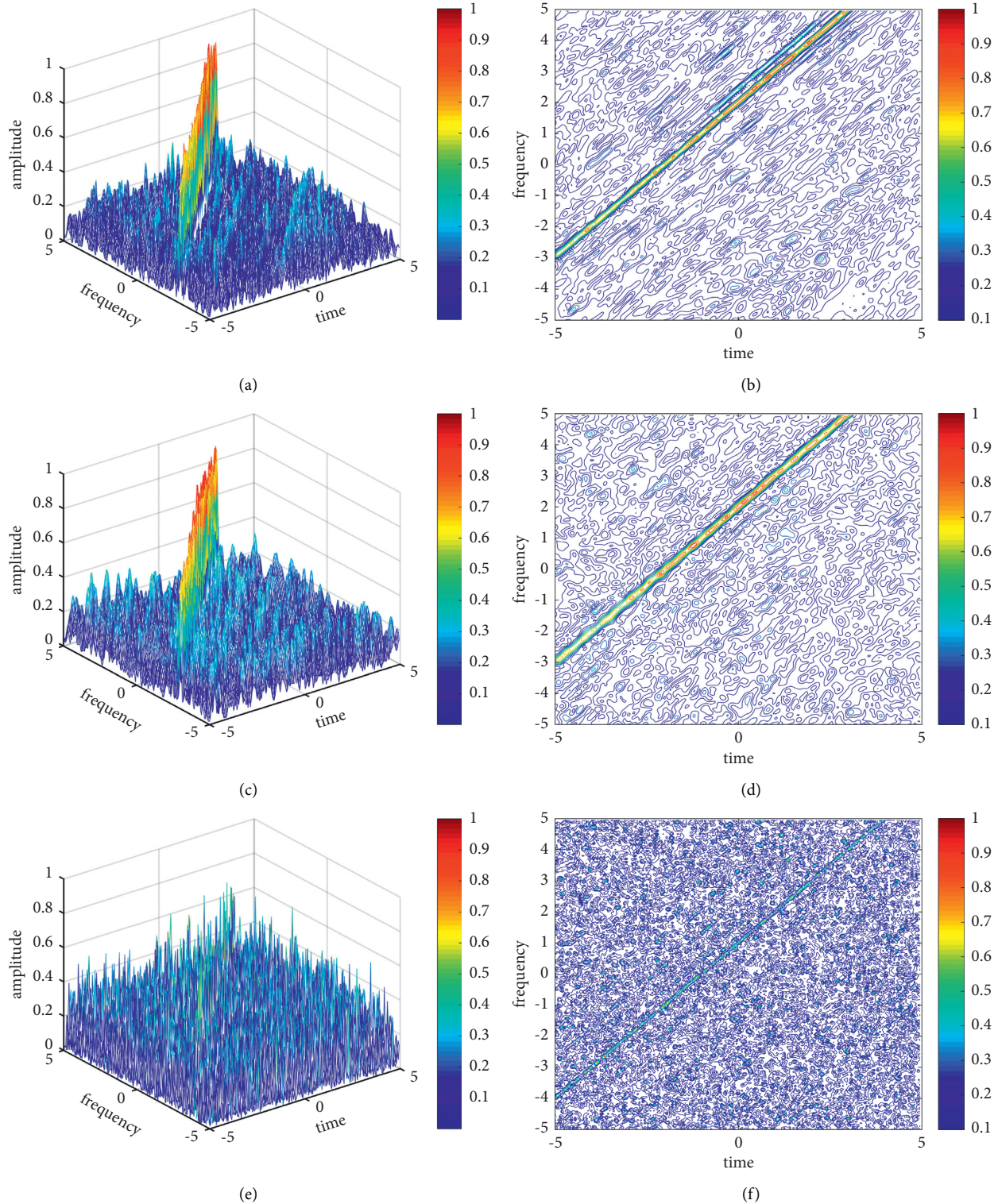(a)

(b)

(c)

(d)

(e)

(f)

FIGURE 1: The detection performance of ICFWD, CICFWD, and WD. The input SNR is -10 dB. The sampling frequency takes 20 Hz. (a) The ICFWD with $\mathbf{A}_1 = (-1, 2; -1, 1)$ and $\mathbf{A} = (1/2, 2; -3/4, -1)$. (b) The ICFWD's contour picture. (c) The CICFWD with $\mathbf{A}_1 = (3/2, 1; -1, 0)$, $\mathbf{A}_2 = (11/6, -1; 1, 0)$, and $\mathbf{A} = (1, 5/2; -4/15, 1/3)$. (d) The CICFWD's contour picture. (e) The WD. (f) The WD's contour picture.
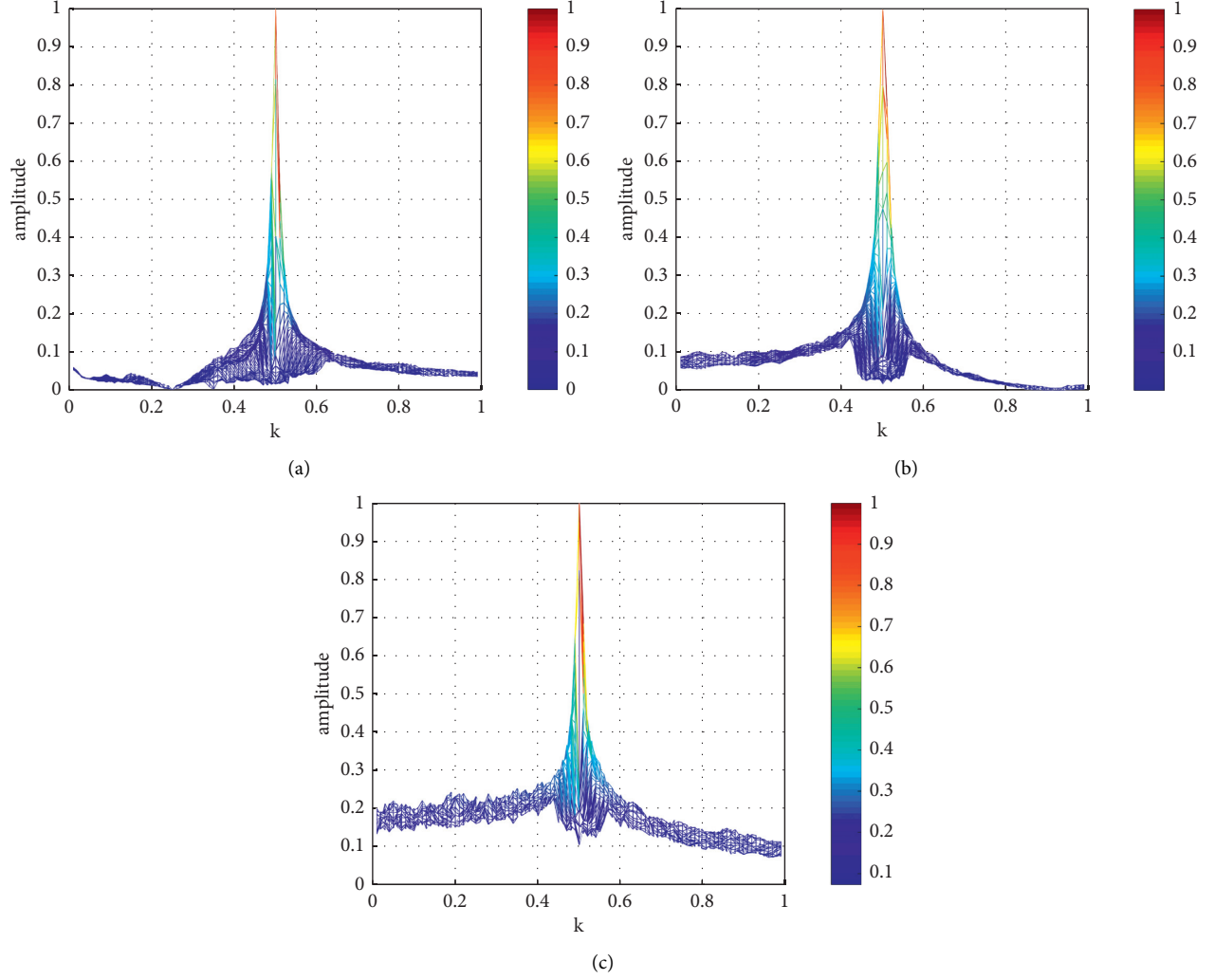
(a)

(b)

(c)

FIGURE 2: The detection performance of RICFWD, RCICFWD, and RWD. The input SNR is −10 dB. The sampling frequency takes 20 Hz. (a) The RICFWD's k-amplitude distribution. (b) The RCICFWD's k-amplitude distribution. (c) The RWD's k-amplitude distribution.

TABLE 1: Computing time of ICFWD and CICFWD in sampling frequencies 5 Hz, 10 Hz, 15 Hz, and 20 Hz.

Sampling frequency (Hz)	Computing time of ICFWD (s)	Computing time of CICFWD (s)
5	0.0482	0.0745
10	0.1110	0.2331
15	0.2259	0.4780
20	0.3918	0.8207

respectively. Similarly, the RT-based ICFWD, abbreviated as the RICFWD, is given by

$$\chi_{\text{RICFWD}}(k,l) = \int \int_{-\infty}^{+\infty} \left| W_f^{\mathbf{A}_1,\mathbf{A}}(t,u) \right|^2 \times \delta \left[u - b \left(\frac{d_1 - 1/(2kb_1 + a_1)}{2b_1} + k \right) t - \frac{l}{2} b \left(\frac{1}{2kb_1 + a_1} + 1 \right) \right] \mathrm{d}t\mathrm{d}u. \tag{28}$$

Figures 2(a)–2(c) plot the k-amplitude distributions of RICFWD, RCICFWD, and RWD, respectively. As it is seen, the ICFWD maintains the same level of output SNR as the CICFWD, and both are higher than the WD's output SNR.

Table 1 records the computing time of ICFWD and CICFWD in four different sampling frequencies 5 Hz, 10 Hz, 15 Hz, and 20 Hz by using MATLAB language (version R2020b) and Acer NoteBook equipped with Intel(R)
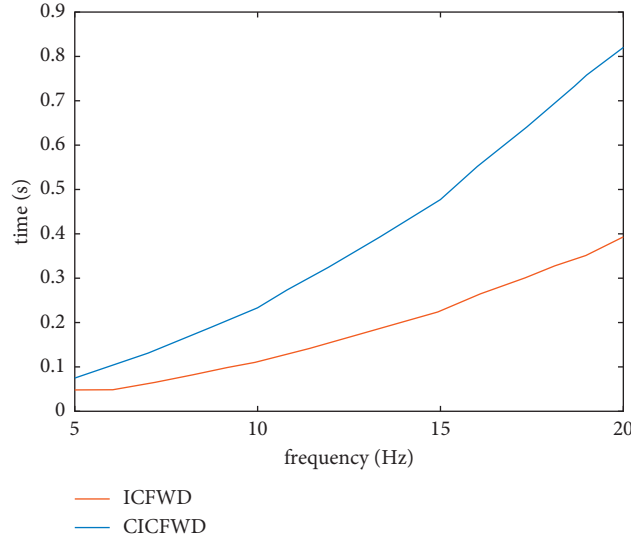
FIGURE 3: The computing speed of ICFWD and CICFWD.

Core(TM) i5-10300H CPU @ 2.50 GHz. The computing time is statistically obtained by averaging over 1000 realizations. Figure 3 plots a comparison of the computing speed of ICFWD and CICFWD. It is clear that the calculating speed of ICFWD can be nearly doubled in comparison with that of CICFWD.

To summarize, the ICFWD exhibits the same level of detection performance as the CICFWD while improving almost a doubling of computing speed.

6. Conclusion

The theory of ICFWD in detecting noisy LFM signals is investigated. By modeling and solving the ICFWD's expectation-SNR optimization problem, the optimal strategy for the determination of the ICFWD's LCT free parameters is definite. It turns out that the ICFWD exhibits the same level of detection performance as the CICFWD but half the computing speed. Although the proposed strategy seems correct and effective, it is not unique. Therefore, the future work will be interested in the uniqueness of the optimal LCT free parameters selection strategy.

Appendix

A. Mathematical Expectation of ICFWD of $f(t) + n(t)$

According to the LCT's linearity property, there is

$$
\begin{aligned}
E\left[W_{f+n}^{\mathbf{A}_1,\mathbf{A}}(t,u)\right] &= E\left[\int_{-\infty}^{+\infty}\left[F_{\mathbf{A}_1}\left(t+\frac{\tau}{2}\right)+N_{\mathbf{A}_1}\left(t+\frac{\tau}{2}\right)\right]\left[f^*\left(t-\frac{\tau}{2}\right)+n^*\left(t-\frac{\tau}{2}\right)\right]\mathscr{K}_{\mathbf{A}}(u,\tau)\mathrm{d}\tau\right] \\
&= E\left[W_f^{\mathbf{A}_1,\mathbf{A}}(t,u)\right] + E\left[W_n^{\mathbf{A}_1,\mathbf{A}}(t,u)\right] \\
&\quad + E\left[\int_{-\infty}^{+\infty}F_{\mathbf{A}_1}\left(t+\frac{\tau}{2}\right)n^*\left(t-\frac{\tau}{2}\right)\mathscr{K}_{\mathbf{A}}(u,\tau)\mathrm{d}\tau\right] \\
&\quad + \mathrm{E}\left[\int_{-\infty}^{+\infty}N_{\mathbf{A}_1}\left(t+\frac{\tau}{2}\right)f^*\left(t-\frac{\tau}{2}\right)\mathscr{K}_{\mathbf{A}}(u,\tau)\mathrm{d}\tau\right].
\end{aligned}
\tag{A.1}
$$

Due to the whiteness of noise, it follows that $\mathrm{E}[n(t)] = \mathrm{E}[n^*(t)] = 0$, from which it derives

$$E\left[\int_{-\infty}^{+\infty} F_{\mathbf{A}_1}\left(t+\frac{\tau}{2}\right)n^*\left(t-\frac{\tau}{2}\right)\mathscr{K}_{\mathbf{A}}(u,\tau)d\tau\right]$$

$$=\int_{-\infty}^{+\infty} F_{\mathbf{A}_1}\left(t+\frac{\tau}{2}\right)E\left[n^*\left(t-\frac{\tau}{2}\right)\right]\mathscr{K}_{\mathbf{A}}(u,\tau)d\tau$$

$$=0,$$

$$E\left[\int_{-\infty}^{+\infty} N_{\mathbf{A}_1}\left(t+\frac{\tau}{2}\right)f^*\left(t-\frac{\tau}{2}\right)\mathscr{K}_{\mathbf{A}}(u,\tau)d\tau\right]$$

$$=\int_{-\infty}^{+\infty} E\left[N_{\mathbf{A}_1}\left(t+\frac{\tau}{2}\right)\right]f^*\left(t-\frac{\tau}{2}\right)\mathscr{K}_{\mathbf{A}}(u,\tau)d\tau \qquad \text{(A.2)}$$

$$=\int_{-\infty}^{+\infty} E\left[\int_{-\infty}^{+\infty} n(\varepsilon)\mathscr{K}_{\mathbf{A}_1}\left(t+\frac{\tau}{2},\varepsilon\right)d\varepsilon\right]f^*\left(t-\frac{\tau}{2}\right)\mathscr{K}_{\mathbf{A}}(u,\tau)d\tau$$

$$=\int_{-\infty}^{+\infty}\left(\int_{-\infty}^{+\infty} E[n(\varepsilon)]\mathscr{K}_{\mathbf{A}_1}\left(t+\frac{\tau}{2},\varepsilon\right)d\varepsilon\right)f^*\left(t-\frac{\tau}{2}\right)\mathscr{K}_{\mathbf{A}}(u,\tau)d\tau$$

$$=0.$$

Because of $E[W_f^{\mathbf{A}_1,\mathbf{A}}(t,u)] = W_f^{\mathbf{A}_1,\mathbf{A}}(t,u)$, equation (A.1) becomes the required result (6).

B. Module of ICFWD's Mathematical Expectation of White Noise

It follows from $E[n(t_1)n^*(t_2)] = D\delta(t_1 - t_2)$ that

$$E\left[N_{\mathbf{A}_1}\left(t+\frac{\tau}{2}\right)n^*\left(t-\frac{\tau}{2}\right)\right] = E\left[\int_{-\infty}^{+\infty} n(\varepsilon)n^*\left(t-\frac{\tau}{2}\right)\mathscr{K}_{\mathbf{A}_1}\left(t+\frac{\tau}{2},\varepsilon\right)d\varepsilon\right]$$

$$=\int_{-\infty}^{+\infty} E\left[n(\varepsilon)n^*\left(t-\frac{\tau}{2}\right)\right]\mathscr{K}_{\mathbf{A}_1}\left(t+\frac{\tau}{2},\varepsilon\right)d\varepsilon$$

$$=D\int_{-\infty}^{+\infty}\delta\left(\varepsilon-t+\frac{\tau}{2}\right)\mathscr{K}_{\mathbf{A}_1}\left(t+\frac{\tau}{2},\varepsilon\right)d\varepsilon \qquad \text{(B.1)}$$

$$=\frac{D}{\sqrt{j2\pi b}}e^{j(a_1+d_1-2)/(2b_1)t^2}e^{j(a_1+d_1+2)/(8b_1)\tau^2}e^{j(d_1-a_1)/(2b_1)t\tau}.$$

Then the expectation of ICFWD of white noise has a form

$$E\left[W_n^{\mathbf{A}_1,\mathbf{A}}(t,u)\right]=\int_{-\infty}^{+\infty} E\left[N_{\mathbf{A}_1}\left(t+\frac{\tau}{2}\right)n^*\left(t-\frac{\tau}{2}\right)\right]\mathscr{K}_{\mathbf{A}}(u,\tau)d\tau$$

$$\qquad \text{(B.2)}$$

$$=\frac{D}{\sqrt{j2\pi b_1}}\frac{1}{\sqrt{j2\pi b}}e^{jd/(2b)u^2}e^{j(a_1+d_1-2)/(2b_1)t^2}\int_{-\infty}^{+\infty} e^{j((a_1+d_1+2)/(8b_1)+(a/2b))\tau^2}e^{j((d_1-a_1)/(2b_1)t-(u/b))\tau}d\tau.$$

For $(a_1 + d_1 + 2)/b_1 \neq -(4a/b)$ by using (15), and subsequently by taking the module, there is the required result (16).

C. Solution of the System of Algebraic Equations (21)

$b^2 (h_1 + 1)^2$ is a function of parameters a_1, b_1, b, since $h_1 = 1/(2\beta b_1 + a_1)$ is a function of parameters a_1 and b_1. Then, the Lagrange function takes

$$
\begin{aligned}
\mathscr{L}(a_1, b_1, b, \lambda) &= f(a_1, b_1, b) + \lambda g(a_1, b_1, b) \\
&= b^2 (h_1 + 1)^2 + \lambda \left(\frac{a}{2b} + \frac{d_1 - h_1}{8b_1} - \frac{\beta}{4} \right).
\end{aligned} \tag{C.1}
$$

Taking its partial derivatives with respect to a_1, b_1, b, λ and setting them to zero yield

$$
\begin{aligned}
\frac{\partial \mathscr{L}}{\partial a_1} &= -h_1^2 \left(2b^2 h_1 + 2b^2 - \frac{\lambda}{8b_1} \right) \\
&= 0, \\
\frac{\partial \mathscr{L}}{\partial b_1} &= -2\beta h_1^2 \left(2b^2 h_1 + 2b^2 - \frac{\lambda}{8b_1} \right) + \frac{\lambda(h_1 - d_1)}{8b_1^2} \\
&= 0, \\
\frac{\partial \mathscr{L}}{\partial b} &= 2b(h_1 + 1)^2 - \frac{\lambda a}{2b^2} \\
&= 0, \\
\frac{\partial \mathscr{L}}{\partial \lambda} &= \frac{a}{2b} + \frac{d_1 - h_1}{8b_1} - \frac{\beta}{4} \\
&= 0.
\end{aligned} \tag{C.2}
$$

Then there are a couple of equations

$$
2b^2 (h_1 + 1) = \frac{\lambda}{8b_1}, \tag{C.3}
$$

$$
2\beta h_1^2 \left(2b^2 h_1 + 2b^2 - \frac{\lambda}{8b_1} \right) = \frac{\lambda(h_1 - d_1)}{8b_1^2}, \tag{C.4}
$$

$$
4b^3 (h_1 + 1)^2 = \lambda a, \tag{C.5}
$$

$$
\frac{2a}{b} + \frac{d_1 - h_1}{2b_1} = \beta. \tag{C.6}
$$

Combining (C.3) and (C.5) gives

$$
h_1 + 1 = \frac{4a}{b} b_1. \tag{C.7}
$$

By substituting (C.3) into the left-hand side of (C.4), there is

$$
h_1 = d_1, \tag{C.8}
$$

and subsequently substituting this relation into the left-hand side of (C.6) yields

$$
\frac{2a}{b} = \beta. \tag{C.9}
$$

With (C.7)–(C.9), there are the required results (22) and (23).

Data Availability

No data were used to support this study.

Conflicts of Interest

The authors declare that they have no financial and personal relationships with other people or organizations that can inappropriately influence the work reported in this study.

Acknowledgments

References

[1] S. A. Collins, "Lens-system diffraction integral written in terms of matrix optics ∗," *Journal of the Optical Society of America*, vol. 60, no. 9, pp. 1168–1177, 1970.

[2] M. Moshinsky and C. Quesne, "Linear canonical transformations and their unitary representations," *Journal of Mathematical Physics*, vol. 12, no. 8, pp. 1772–1780, 1971.

[3] J. J. Healy, M. A. Kutay, H. M. Ozaktas, and J. T. Sheridan, Eds., *Linear Canonical Transforms: Theory and Applications*, Springer, New York, NY, USA, 2016.

[4] T. Z. Xu and B. Z. Li, *Linear Canonical Transforms and its Applications*, Science Press, Beijing, China, 2013.

[5] Z. C. Zhang, "Choi-Williams distribution in linear canonical domains and its application in noisy LFM signals detection," *Communications in Nonlinear Science and Numerical Simulation*, vol. 82, Article ID 105025, 2020.

[6] Z. C. Zhang, "Variance analysis of linear canonical Wigner distribution," *Optik*, vol. 212, Article ID 164633, 2020.

[7] Z. C. Zhang, "Variance analysis of noisy LFM signal in linear canonical Cohen's class," *Optik*, vol. 216, Article ID 164610, 2020.

[8] Z. C. Zhang, S. Z. Qiang, X. Jiang, P. Y. Han, X. Y. Shi, and A. Y. Wu, "Linear canonical Wigner distribution of noisy LFM signals via variance-SNR based inequalities system analysis," *Optik*, vol. 237, Article ID 166712, 2021.

[9] M. J. Bastiaans, "The Wigner distribution function applied to optical signals and systems," *Optics Communications*, vol. 25, no. 1, pp. 26–30, 1978.

[10] L. Stankovic, S. Stankovic, and M. Dakovic, "From the STFT to the Wigner distribution [lecture notes]," *IEEE Signal Processing Magazine*, vol. 31, no. 3, pp. 163–174, 2014.

[11] Z. C. Zhang, X. Jiang, S. Z. Qiang et al., "Scaled Wigner distribution using fractional instantaneous autocorrelation," *Optik*, vol. 237, Article ID 166691, 2021.

[12] L. Cohen, *Time-Frequency Analysis*, Prentice-Hall PTR, New Jersey, NJ, USA, 1995.

[13] Y. Luo, L. Zhang, and H. Ruan, "An acquisition algorithm based on FRFT for weak GNSS signals in a dynamic environment," *IEEE Communications Letters*, vol. 22, no. 6, pp. 1212–1215, 2018.

[14] X. Fu, B. Wang, M. Xiang, S. Jiang, and X. Sun, "Residual RCM correction for LFM-CW mini-SAR system based on fast-time split-band signal interferometry," *IEEE Transactions on Geoscience and Remote Sensing*, vol. 57, no. 7, pp. 4375–4387, 2019.

[15] S. C. Pei and J. J. Ding, "Relations between fractional operations and time-frequency distributions, and their applications," *IEEE Transactions on Signal Processing*, vol. 49, no. 8, pp. 1638–1655, 2001.

[16] R. F. Bai, B. Z. Li, and Q. Y. Cheng, "Wigner-Ville distribution associated with the linear canonical transform," *Journal of Applied Mathematics*, vol. 2012, Article ID 740161, 14 pages, 2012.

[17] Z.-C. Zhang, "New Wigner distribution and ambiguity function based on the generalized translation in the linear canonical transform domain," *Signal Processing*, vol. 118, pp. 51–61, 2016.

[18] Z.-C. Zhang, "Unified Wigner-Ville distribution and ambiguity function in the linear canonical transform domain," *Signal Processing*, vol. 114, pp. 45–60, 2015.

[19] Z. Zhang, D. Li, Y. Chen, and J. Zhang, "Linear canonical Wigner distribution of noisy LFM signals via multiobjective optimization analysis involving variance-SNR," *IEEE Communications Letters*, vol. 25, no. 2, pp. 546–550, 2021.

[20] Z. Zhang and M. Luo, "New integral transforms for generalizing the Wigner distribution and ambiguity function," *IEEE Signal Processing Letters*, vol. 22, no. 4, pp. 460–464, 2015.

[21] Z. Zhang, "Linear canonical Wigner distribution based noisy LFM signals detection through the output SNR improvement analysis," *IEEE Transactions on Signal Processing*, vol. 67, no. 21, pp. 5527–5542, 2019.

[22] Z. Zhang, "The optimal linear canonical Wigner distribution of noisy linear frequency-modulated signals," *IEEE Signal Processing Letters*, vol. 26, no. 8, pp. 1127–1131, 2019.

[23] J. Ma, R. Tao, Y. Li, and X. Kang, "Fractional power spectrum and fractional correlation estimations for nonuniform sampling," *IEEE Signal Processing Letters*, vol. 27, pp. 930–934, 2020.

[24] J. Shi, J. Zheng, X. Liu, W. Xiang, and Q. Zhang, "Novel short-time fractional Fourier transform: theory, implementation, and applications," *IEEE Transactions on Signal Processing*, vol. 68, pp. 3280–3295, 2020.

[25] J. Ma, R. Tao, Y. Li, and X. Kang, "Fractional spectrum analysis for nonuniform sampling in the presence of clock jitter and timing offset," *IEEE Transactions on Signal Processing*, vol. 68, pp. 4148–4162, 2020.

[26] J. Shi, X. Liu, W. Xiang, M. Han, and Q. Zhang, "Novel fractional wavelet packet transform: theory, implementation, and applications," *IEEE Transactions on Signal Processing*, vol. 68, pp. 4041–4054, 2020.

[27] Y.-M. Li, D. Wei, and L. Zhang, "Double-encrypted watermarking algorithm based on cosine transform and fractional Fourier transform in invariant wavelet domain," *Information Sciences*, vol. 551, pp. 205–227, 2021.

[28] L. Zhao, J. T. Sheridan, and J. J. Healy, "Unitary algorithm for nonseparable linear canonical transforms applied to iterative phase retrieval," *IEEE Signal Processing Letters*, vol. 24, no. 6, pp. 814–817, 2017.

[29] J. Shi, X. Liu He, L. He, M. Han, Q. Li, and N. Zhang, "Sampling and reconstruction in arbitrary measurement and approximation spaces associated with linear canonical transform," *IEEE Transactions on Signal Processing*, vol. 64, no. 24, pp. 6379–6391, 2016.

[30] J. Shi, X. P. Liu, F. G. Yan, and W. B. Song, "Error analysis of reconstruction from linear canonical transform based sampling," *IEEE Transactions on Signal Processing*, vol. 66, no. 7, pp. 1748–1760, 2018.

[31] J. Shi, X. Liu, Y. Zhao, S. Shi, X. Sha, and Q. Zhang, "Filter design for constrained signal reconstruction in linear canonical transform domain," *IEEE Transactions on Signal Processing*, vol. 66, no. 24, pp. 6534–6548, 2018.

[32] D. Wei, W. Yang, and Y.-M. Li, "Lattices sampling and sampling rate conversion of multidimensional bandlimited signals in the linear canonical transform domain," *Journal of the Franklin Institute*, vol. 356, no. 13, pp. 7571–7607, 2019.

[33] D. Wei and Y.-M. Li, "Convolution and multichannel sampling for the offset linear canonical transform and their applications," *IEEE Transactions on Signal Processing*, vol. 67, no. 23, pp. 6009–6024, 2019.

[34] Q. Feng, B.-Z. Li, and J.-M. Rassias, "Weighted Heisenberg-Pauli-Weyl uncertainty principles for the linear canonical transform," *Signal Processing*, vol. 165, pp. 209–221, 2019.

[35] W. B. Gao and B. Z. Li, "Uncertainty principles for the short-time linear canonical transform of complex signals," *Digital Signal Processing*, vol. 111, Article ID 102953, 2021.

[36] A. Mefleh, *Contributions to Extreme Value Theory: Trend Detection for Heteroscedastic Extremes*, Universite Bourgogne Franche-Comte, Besançon, France, 2018.

[37] K. E. Browne and R. J. Burkholder, "Nonlinear optimization of radar images from a through-wall sensing system via the Lagrange multiplier method," *IEEE Geoscience and Remote Sensing Letters*, vol. 9, no. 5, pp. 803–807, 2012.

[38] F. Scholkmann, J. Boss, and M. Wolf, "An efficient algorithm for automatic peak detection in noisy periodic and quasi-periodic signals," *Algorithms*, vol. 5, no. 4, pp. 588–603, 2012.

[39] Y. Wang, B. Xu, G. Sun, and S. Yang, "A two-phase differential evolution for uniform designs in constrained experimental domains," *IEEE Transactions on Evolutionary Computation*, vol. 21, no. 5, pp. 665–680, 2017.

[40] M. S. Wang, A. K. Chan, and C. K. Chui, "Linear frequency-modulated signal detection using radon-ambiguity transform," *IEEE Transactions on Signal Processing*, vol. 46, no. 3, pp. 571–586, 1998.